Manuscript refereed by Mr John Dunkley, Atomising Systems Ltd

New Iron Powder for Low Density Applications

François Chagnon

Rio Tinto Metal Powders
1655 Marie-Victorin
Sorel-Tracy
Quebec, Canada
J3R 4R4

ABSTRACT

Although most of the new PM applications require high density to withstand demanding loads, many parts are still produced in a density range of 6.0 to 6.6 g/cm³. For such applications, high green strength is a key factor to avoid green cracks during compaction and handling before sintering. These parts must also show good dimensional stability during sintering. A study has been carried out to evaluate the behaviour of various powder grades during sintering. F-0005 and FC-0205 mixes were prepared and pressed to a green density of 6.4 g/cm³. Sintered properties were evaluated and dimensional behaviour characterized by dilatometry. Also, compressibility and green strength were determined at 275, 480 and 690 MPa using a mix with 0.75% EBS wax.

Results showed that with proper modification of particle morphology and particle size distribution, the dimensional change can be modified and the green strength improved.

INTRODUCTION

Even if most of the new parts developed in the PM market need high density to resist higher load in operation, many PM parts are still produced in a density range of 6.0 to 6.6 g/cm³ because of the need for residual porosity or to reduce weight. For such applications, green strength at low density is a key parameter to avoid green cracks during compaction and handling before sintering. For these applications, sponge iron manufactured by oxide reduction [1] is very popular and widely used in the PM industry. Low apparent density powders can also be produced from water granulated cast iron powder, which is subsequently ball milled to a specific particle size distribution before decarburization [1,2] or by water atomization with specific manufacturing conditions to favour powder agglomeration during annealing [3]. However, even if these powders are intended to be used in similar applications, because of the different manufacturing processes, green and sintered properties may differ. As an example, ATOMET 24 and ATOMET 25 produced by Rio Tinto Metal Powders exhibit significantly lower growth values comparatively to sponge iron powder, table 1. Indeed, in term of dimensional change, sponge iron behaves more similarly to that of water atomized steel powders. On the other hand, water atomized steel powders generally show very low green strength at low density because of their better compressibility. Therefore, a R&D project has been initiated with the objective of better understanding the behaviour during sintering specimens pressed with these powders and develop a new powder with excellent green strength at low density but with dimensional behaviour close to that of water atomized steel powders and sponge iron powder.

	Dimensional change, % vs die size, % (% vs green size)
ATOMET 24	**+0.21 (-0.03)**
ATOMET 1001	**+0.28 (+0.11)**
Sponge iron powder	**+0.33 (+0.11)**

Table 1. Dimensional change of specimens pressed from three different powders (mix containing 0.9 % graphite and 2% copper pressed at 6.8 g/cm³).

EXPERIMENTAL PROCEDURE

Three different powder grades were used in this study: ATOMET 22 (powder A), a new iron powder developed for low density applications with dimensional behaviour similar to that of traditional sponge iron powder, ATOMET 24 (powder B) and ATOMET 25 (powder C). Table 2 summarizes the typical chemical and physical properties of these three grades. Powder A, the new powder grade, shows the lowest carbon and oxygen concentrations, a coarser particle size distribution and the lowest apparent density together with powder B. Powder C shows the highest apparent density and -325 mesh fraction. For powder A, by proper adjustments of the production parameters, particle morphology has been modified to produce powders with irregular particle shape to maintain a low apparent density and hence a high green strength together with a lesser concentration of –325 mesh as compared to powders B and C. Also, these modifications make possible to achieve larger growth values during sintering.

Powder	C, %	O, %	S, %	+70 mesh, %	-70/+100 mesh, %	-100/+325 mesh, %	-325 mesh, %	Apparent density, g/cm³	Flow, s/50 g
A	0.005	0.15	0.003	0	6.2	71.8	22.0	2.46	29
B	0.007	0.20	0.007	0.1	3.6	70.5	25.8	2.46	29
C	0.024	0.16	0.008	0.1	0.8	67.2	31.9	2.54	30

Table 2. Chemical and physical properties of the three powder grades used in this study.

In the first part of the study, the green properties of each grade were evaluated with TRS specimens (3.18 X 1.27 X 0.64 cm) pressed at 275, 480 and 690 MPa from mixes containing 0.75% EBS wax. In the second part of the study, the dimensional change behaviour of each grade was evaluated using rectangular specimens of 2.5 X 0.6 X 0.6 cm pressed at 6.4 g/cm³ with die wall lubrication from mixes containing either 0.7% graphite or with 0.7% graphite and 2% copper. These specimens were sintered in a 90% nitrogen based atmosphere in a dilatometer with a heating rate of 20°C/min., a holding time of 30 minutes at 1125°C and a cooling rate of 10°C/min. Finally, the sintered properties were evaluated using TRS specimens (3.18 X 1.27 X 0.64 cm) and dog bones specimens at 6.4 g/cm³ with the same mix composition but with 0.75% EBS wax. Sintering was carried out in a mesh belt furnace at 1125°C for 25 minutes in a 90% nitrogen based atmosphere. The dimensional change from die size and green size as well as the tensile and yield strengths, elongation and apparent hardness were evaluated for each mix composition. Finally the microstructure was observed after Nital etching at 200 X by optical microscopy.

RESULTS AND DISCUSSION

Figure 1 illustrates the variation of green density with compacting pressure and green strength with green density of specimens pressed with powders A, B and C with 0.75% EBS wax. Powder B shows the best compressibility, slightly better than that of powder A but significantly better than powder C. At 500 MPa, specimens pressed with powder B show a green density of about 6.82 g/cm³, those pressed with powder A, 6.77 g/cm³ and those with powder C, 6.72 g/cm³. On the other hand, for a given green density, specimens pressed with powder A show the highest green strength values while those pressed with powder B and C show similar green strengths. As an example, at 6.4 g/cm³, specimens pressed with powder A show a green strength of 14.5 MPa and those pressed with powder B and C, 12 MPa. This increase in green strength for powder A can be related to a change in particle morphology as shown in figure 2. The shape of powder A, the new powder grade, is irregular with fewer small particles with a rounder shape, while powder B shows a larger quantity of very small particles. The coarser ones are also less irregular than that of powder A.

Figure 3 illustrates the dilatometry curves of specimens pressed with the three powder grades from the mixes with 0.7% graphite and 0.7% graphite and 2% Cu. For the Fe-C steels, a slight change of the slope occurs at around 750°C for materials B and C and at around 770°C for material A. For the Fe-C-Cu steels, this change in the slope occurs at a slightly lower temperature, 710°C for material A and 680°C for materials B and C. The phase transformation for both the Fe-C and Fe-C-Cu steels starts at around 860-870°C for the three materials and ends at about 930°C for the three powders. The temperature where the end of carbon diffusion occurs is similar for all materials, around 1030°C. Copper melting occurs at around 1085°C for the Fe-C-Cu steels but slightly larger growth is observed with material A, +0.17% vs +0.16% for material B and +0.14% for material C. The degree of shrinkage at the 1025°C isotherm is similar for the three materials, within -0.10 to -0.11% for the Fe-C steels and -0.07 to -0.09% the Fe-C-Cu steels. The phase transformation on cooling for the Fe-C steels starts at about 720-730°C and ends at about 670-680°C for all materials. For the Fe-C-Cu steels, the phase transformation starts at about 700°C and ends at about 640-650°C. Its is worth noting that the shrinkage observed just before the phase transformation and during the phase transformation on heating is lower for material A compared to the two other materials and explains most of the difference in dimensional change results. Another part of the difference for the Fe-C-Cu steels can be related to copper growth at around 1085°C, which is larger for material A compared to materials B and C.

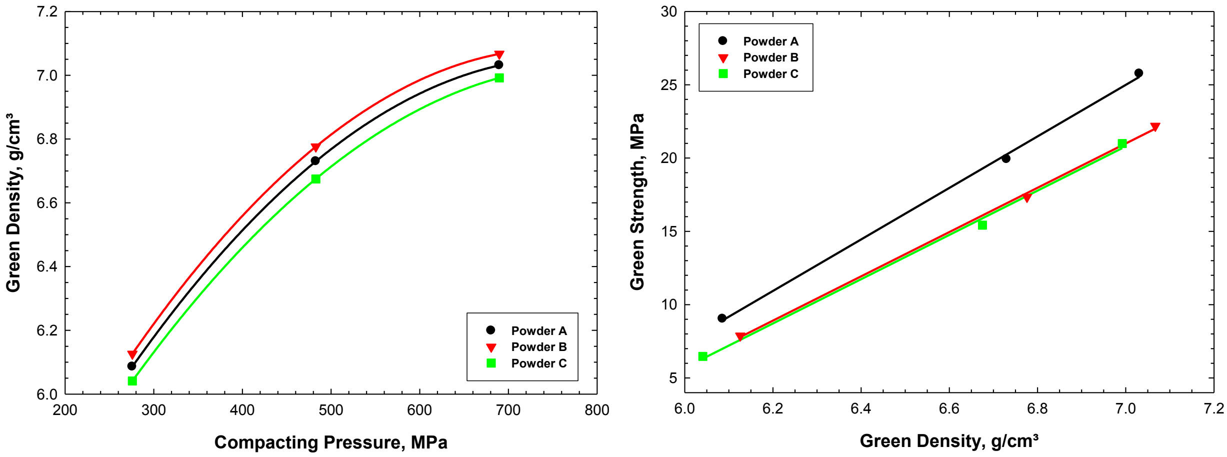

A B

Figure 1. Variation of green density with compacting pressure (A) and green strength with green density (B) of specimens pressed with the three powder grades (mixes containing 0.75% EBS wax).

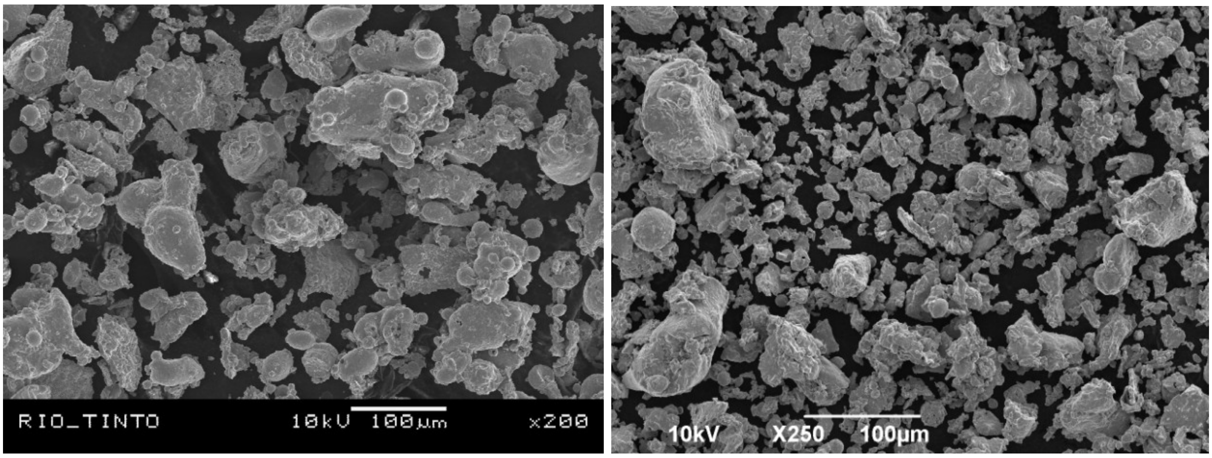

Powder A Powder B

Figure 2. Particle morphology of Powder A and Powder B.

Table 3 summarizes the sintered properties of specimens pressed at 6.4 g/cm³ from mixes made with powders A, B and C with either 0.7% graphite or 0.7% graphite and 2% copper. After sintering, the carbon concentrations in the specimens were 0.60%, on average. Figure 4 compares the dimensional change from both the green and die size of specimens pressed at 6.4 g/cm³ from the various powder mixes with 0.7% graphite and either 0 or 2% Cu. For both mix formulations, material A shows lower shrinkage or larger growth values than materials B and C. On average, the difference is +0.04% vs green size and +.05% vs die size for the Fe-C steels, and +0.06 and +0.07%, respectively, for the Fe-Cu-C.

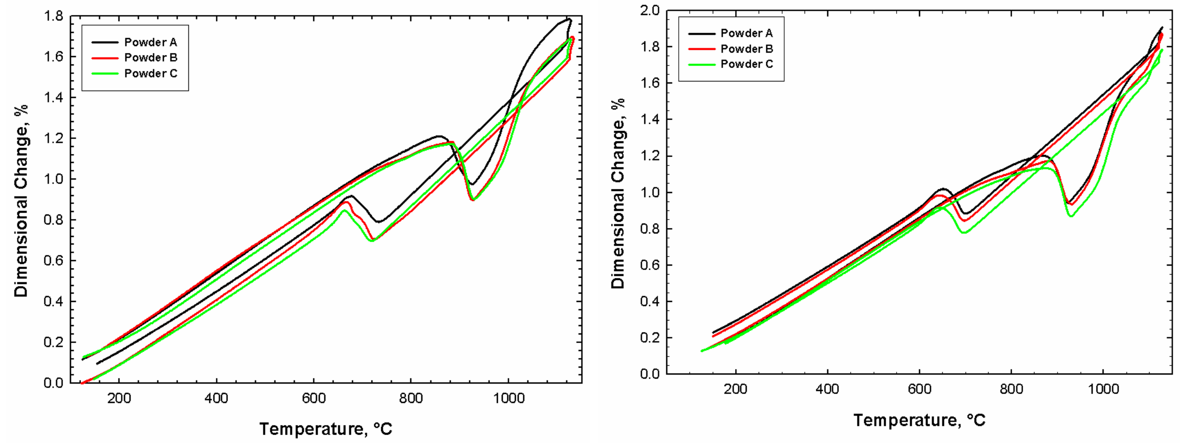

0.6% C | 0.% C-2% Cu

Figure 3. Dilatometry profiles of material A, B and C with 0.6% C and 0.6% C and 2% Cu.

	Powder A		Powder B		Powder C	
	0.6%C-0%Cu	0.6%C-2%Cu	0.6%C-0%Cu	0.6%C-2%Cu	0.6%C-0%Cu	0.6%C-2%Cu
Dimensional change, % vs d.s.	0.04	0.25	-0.02	0.19	0.01	0.19
Dimensional change, % vs g.s.	-0.11	0.11	-0.17	0.04	-0.14	0.04
Tensile strength, MPa	286	388	271	365	261	373
Yield strength, MPa	244	344	226	319	228	328
Elongation, %	1.5	1.0	1.9	1.1	1.3	1.0
Apparent hardness, HRB	45.7	63.7	44.3	59.0	44.0	60.7
Sintered carbon, %	0.60	0.60	0.56	0.60	0.61	0.61

Table 3. Sintered properties of Fe-C and Fe-C-Cu steels from materials A, B and C (green density of 6.4 g/cm³).

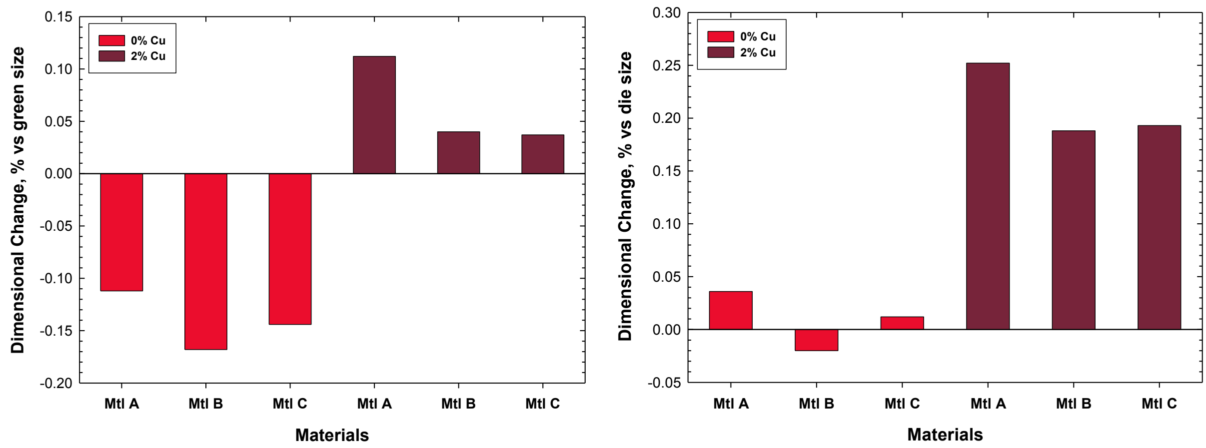

Green size | Die size

Figure 4. Dimensional change from green and die size of materials A, B and C with 0.6%C and either 0 or 2%Cu (green density of 6.4 g/cm³).

Figure 5 compares the tensile and yield strengths, elongation and apparent hardness values reached with the various materials at 6.4 g/cm³. For both the Fe-C and Fe-Cu-C steels, material A shows higher tensile and yield strength, about 20 MPa on average, and apparent hardness values, about 3 HRB on average, than materials B and C.

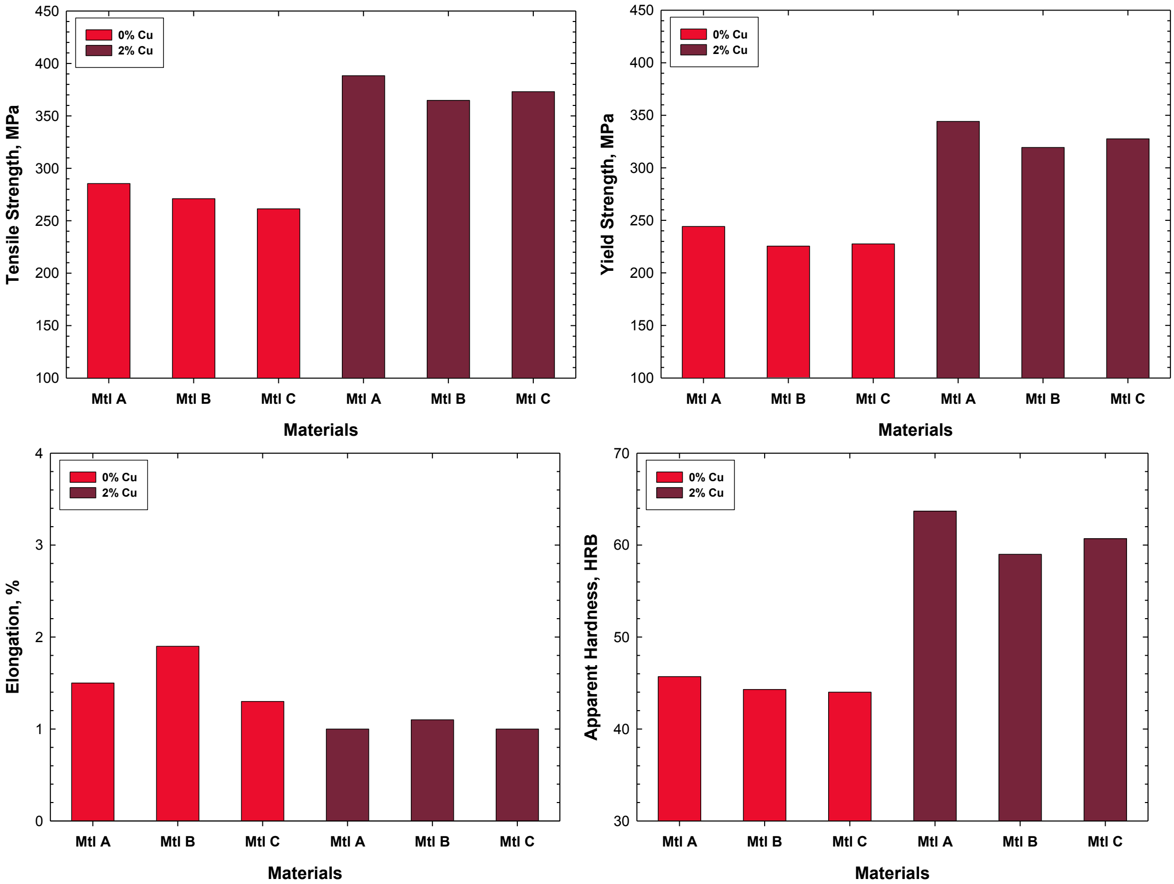

Figure 5. Tensile and yield strengths, elongation and apparent hardness of materials A, B and C with 0.6%C and either 0 or 2.0%Cu (green density of 6.4 g/cm³).

Figure 6 shows typical etched microstructures of materials A, B and C with either 0.6% C or 0.6% C and 2% Cu. The microstructure is very similar for the various materials and is composed of pearlite and ferrite, in line with the carbon concentration. It is worth noting that the porosity distribution differs compared to that of traditional sponge iron. Indeed, sponge iron is produced from 100% iron oxides as raw material, which is subsequently reduced. All the three powders, A, B and C, are in fact composed of dense and porous particles. The dense particles are more typical of water atomized powders while the porous ones are more comparable to that of iron oxide reduced powders. During the manufacturing of these different powder grades, particle size and morphology of the dense particles are modified while the quantity of porous particles, which is agglomerated to the denser ones is varied to reach specific apparent density.

CONCLUSIONS

A new low apparent density iron powder grade has been developed with excellent green strength at low density. The particle size distribution and morphology have been modified to increase green strength and achieve dimensional change response during sintering similar to that of traditional sponge iron powders.

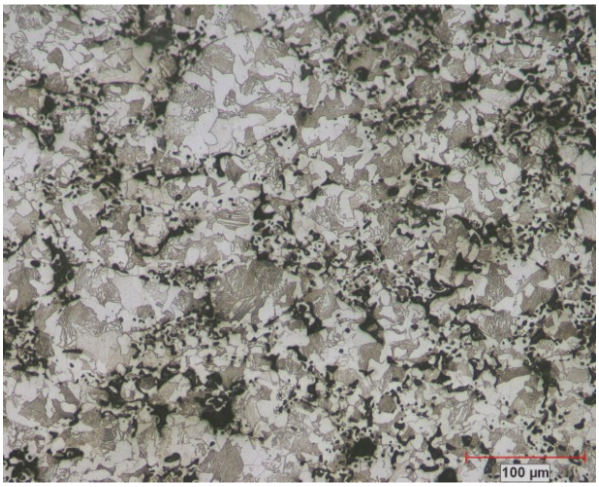

Mtl A; 0.6%C

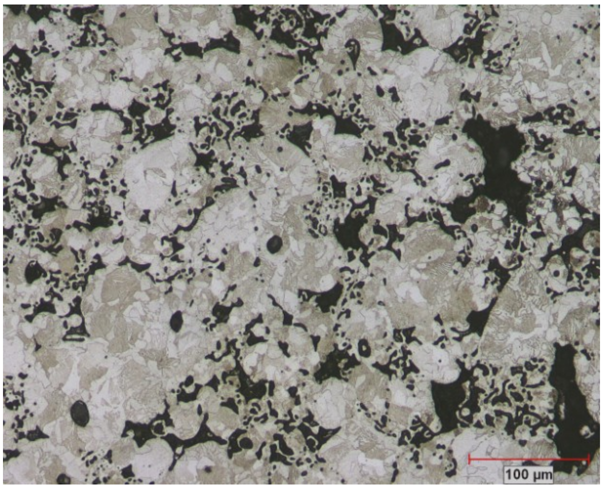

Mtl A; 0.6%C-2% Cu

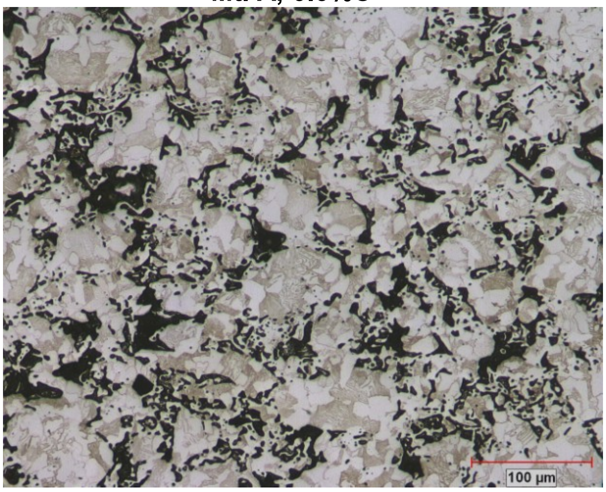

Mtl B; 0.6%C

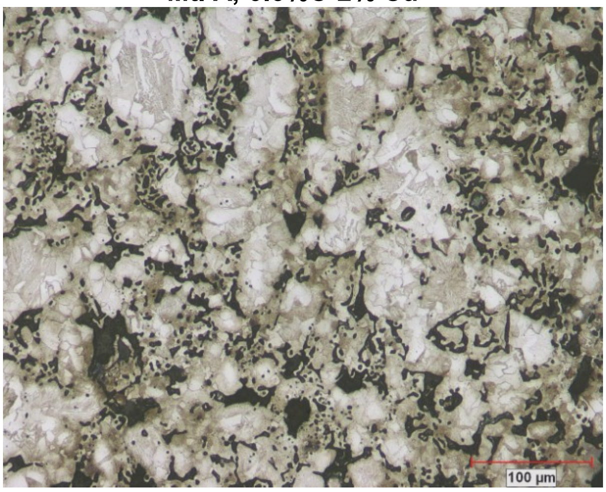

Mtl B; 0.6%C-2% Cu

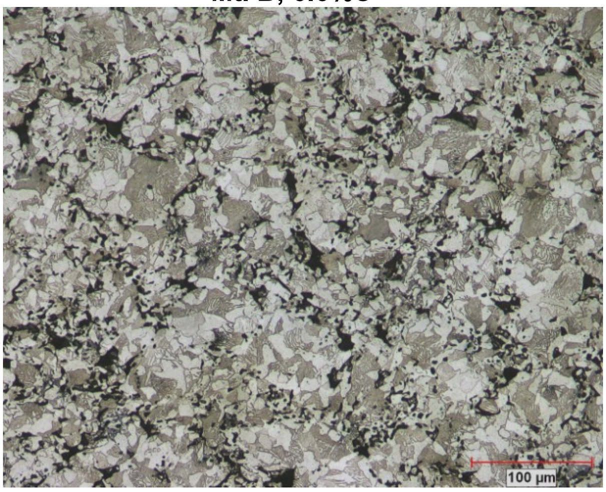

Mtl C; 0.6%C

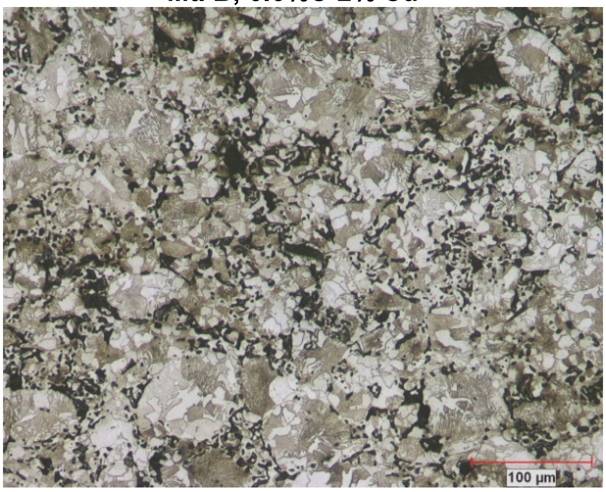

Mtl C; 0.6%C.-2% Cu

Figure 6. Etched microstructure of materials A, B and C with 0.6%C and either 0 or 2%Cu (natal etched; 200X).

REFERENCES

1. Basic PM Short Course, July 27-29, 2009, State College, PA, MPIF.
2. Rio Tinto Metal Powders' flowchart.
3. Hanejko, F. and Rutz, H.; "A New Atomized Low Apparent Density "Sponge Like" Iron Powder", Proceedings of EURO PM2009, EPMA, Shrewsbury, UK, 2009.